



Article

# Mathematical Identification Analysis of a Fractional-Order Delayed Model for Tuberculosis

Slavi Georgiev <sup>1,2</sup>

<sup>1</sup> Department of Informational Modeling, Institute of Mathematics and Informatics, Bulgarian Academy of Sciences, 1113 Sofia, Bulgaria; sggeorgiev@uni-ruse.bg or sggeorgiev@math.bas.bg; Tel.: +359-82-888-725

<sup>2</sup> Department of Applied Mathematics and Statistics, Faculty of Natural Sciences and Education, University of Ruse, 8 Studentska Str., 7004 Ruse, Bulgaria

**Abstract:** Extensive research was conducted on the transmission dynamics of tuberculosis epidemics during its reemergence from the 1980s to the early 1990s, but this global problem of investigating tuberculosis spread dynamics remains of paramount importance. Our study utilized a fractional-order delay differential model to study tuberculosis transmission, where the time delay in the model was attributed to the disease's latent period. What is more, this model accounts for endogenous reactivation, exogenous reinfection, and treatment of tuberculosis. The model qualitative properties and the basic reproduction number were analyzed. The primary goal of the study was to recover the important dynamic parameters of tuberculosis. Our understanding of these complex processes leverages the efficacy of efforts for controlling the disease, forecasting future dynamics, and applying further appropriate strategies to prevent its spread. The calibration itself was carried out via minimization of a quadratic cost functional. Computational simulations demonstrated that the algorithm is capable of working with noisy real data.

**Keywords:** tuberculosis; epidemic modeling; inverse problems; basic reproduction number; caputo derivative

**MSC:** 34A08; 34A55; 65L09; 92D25; 92D30



**Citation:** Georgiev, S. Mathematical Identification Analysis of a Fractional-Order Delayed Model for Tuberculosis. *Fractal Fract.* **2023**, *7*, 538. <https://doi.org/10.3390/fractalfract7070538>

Academic Editor: Ivanka Stamova

Received: 8 May 2023

Revised: 2 July 2023

Accepted: 7 July 2023

Published: 12 July 2023



**Copyright:** © 2023 by the author. Licensee MDPI, Basel, Switzerland. This article is an open access article distributed under the terms and conditions of the Creative Commons Attribution (CC BY) license (<https://creativecommons.org/licenses/by/4.0/>).

## 1. Introduction

Tuberculosis, the highly infectious disease caused by the bacterium *Mycobacterium tuberculosis* (MTB), remains a significant health challenge worldwide, particularly in developing countries. This contagious disease is a major cause of mortality and continues to pose a serious threat to public health. MTB can easily spread via respiratory contact as an infected individual coughs, sneezes, spits, or speaks. The disease is characterized by various symptoms, including high fever accompanied by chills, chronic cough, night sweats, nail clubbing, weight loss, and fatigue. As TB is a life-threatening disease, it is crucial to identify and treat the illness at an early stage, to prevent further transmission and improve patient outcomes. The current global situation demands greater efforts towards TB awareness, prevention, and treatment strategies, particularly in countries with high incidence rates.

TB is a highly prevalent infectious disease and is responsible for a significant number of deaths worldwide. It is considered the second leading cause of death caused by an infectious disease globally. Only in 2019, almost 1.2 million people died from TB, and more than 10.3 million people were infected worldwide. The disease primarily affects the lungs, but it can also spread to other parts of the body, such as the circulatory system, central nervous system, genital–urinary system, joints, bones, and skin. Hence, it is important to diagnose and treat TB promptly, to prevent the spread of the disease and mitigate its impact on affected individuals.

Studying disease dynamics remains crucial. TB exhibits complex dynamics, such as latency periods, super-spreading events, and the development of drug resistance. Thus, modeling the disease spread provides us with an understanding of these complex processes. Having gained knowledge about the dynamics, this could be used for predicting the spread within a population over time. Needless to say, this could help public health authorities formulate appropriate strategies to control the spread. What is more, using models, the effect of various interventions on disease dynamics could be assessed, including vaccination, treatment, quarantine, etc. All these factors motivated us to perform the current study, where we formulate a compartmental ODE model, suggest an algorithm to calibrate it, and we fit the model to real-world data.

One of the most powerful approaches for modeling and subsequently controlling such a disease is mathematical modeling. A large class of models focus on transmission dynamics, which explain how waves develop, spread, and evanesce. Mathematical models, as important tools in the study of infectious diseases, provide valuable insights into disease transmission and control. Researchers have developed numerous models to study the dynamics of TB. These models can help to identify effective strategies for preventing the spread of TB and reducing its impact on public health. By analyzing data on TB transmission and disease progression, mathematical models can also help to predict future trends in TB incidence and guide public health interventions. These models are essential for understanding the complex dynamics of TB and developing evidence-based policies to combat the disease.

The SIR (susceptible-infected-removed) compartment model, first suggested in 1927 [1], is considered the first contemporary attempt to model the spread of an infectious disease. Later, many extensions and generalizations were developed. Compartment models are heavily used in modeling epidemics [2,3]. We mention a small part of these studies, dedicated primarily to tuberculosis. In 1962, a TB model was suggested by [4], and a couple of years later, a compartment model was proposed in [5]. In [6], the authors developed a two-stratum model for TB dynamics, distinguishing between fast and slow progressors to active disease. This model highlighted the importance of latency in TB transmission dynamics. An age-structured model was used to differentiate between primary infection and reinfection in TB transmission in [7]. The study underlined the significance of age-related factors and reinfection in TB epidemiology. In the paper in [8], the authors used a compartmental ODE model to simulate the spread of TB under different treatment strategies. They concluded that the WHO's DOTS strategy could significantly reduce TB incidence and mortality. In the study in [9], the authors used a stochastic compartmental model to demonstrate the potential impact of treating latent TB infection. This work underscored the importance of considering latency in TB control efforts. The authors of [10] incorporated drug resistance into a TB model, showing that less fit drug-resistant strains can persist and eventually predominate under standard treatment policies, which was an important contribution to understanding the dynamics of drug-resistant TB. In [11], a compartmental model was used to simulate the spread of extensively drug-resistant TB in South African hospitals. They found that implementing infection control measures could greatly reduce transmission. A complex multi-compartment model that included HIV co-infection and various forms of drug-resistant TB was used in [12]. This model was used to analyze different control strategies, demonstrating the necessity of including these factors in models used in high-burden settings. The authors of [13] used compartmental models to inform policy decisions related to TB control in South Africa. They demonstrated the potential of model-based analysis for guiding resource allocation and intervention planning in a high-burden setting. In [14], the authors developed a model to estimate the global burden of latent multidrug-resistant TB. They found that the number of individuals with latent MDR-TB is substantial and increasing, highlighting the need for new tools and strategies for diagnosing and treating latent MDR-TB. The study in [15] presented a six-compartment deterministic model, to analyze the effects of vaccination on TB dynamics within a population, establishing local asymptotic stability when the effective reproduction number is less than one. The results

underscored the significance of reducing contact with infected individuals and increasing the vaccination rate with an effective vaccine, demonstrating these as key strategies for decreasing the TB burden in a population. A random differential equation system was applied to a mathematical model of tuberculosis transmission in [16], investigating the randomness of disease spread by analyzing expected compartment sizes and coefficients of variations. The sensitivity of the basic reproduction number to parameter changes was also explored, using the forward normalized sensitivity index, with simulations conducted to assess random dynamics of disease transmission.

A more detailed review of mathematical approaches to the modeling and control of TB disease performed over the past century can be found in [17]. Some of the recent studies include [18], where seasonal effects are included, and [19], where a fractional-order TB model with age structure was considered. TB models with vaccination effectiveness were considered in [20].

In the study of [21], a mathematical model was studied for the co-infection of tuberculosis and COVID-19 using the Atangana–Baleanu fractal–fractional operator, considering compartments for recovery from both diseases. They confirmed the existence and uniqueness of a model solution through a fixed-point approach, investigated the Ulam–Hyers stability, and validated the model using Lagrange interpolation polynomial in a numerical scheme, comparing different values of fractional and fractal orders. In [22], the authors proposed a mathematical model for investigating the impact of COVID-19 on TB, providing evidence that TB patients have a higher chance of contracting SARS-CoV-2. Using stability analysis, optimal control theory, and sensitivity analysis, they highlighted the system's endemic equilibrium point, bifurcation behavior, and the key role of the transmission rate in controlling the dynamics of both diseases, confirming that controlling this rate can mitigate COVID-19 and TB infections. In [23], a deterministic mathematical model for the co-infection of COVID-19 and TB was formulated and analyzed, to understand the co-dynamics and impact of each disease within a population, while considering factors such as vaccine efficacy and vaccination rate. Obviously, when the basic reproduction numbers for both diseases are below one, the population reaches a stable disease-free state; however, the authors also found that, while COVID-19 incidence decreases with co-infection prevalence, the burden of tuberculosis on the human population increases, emphasizing the importance of controlling both diseases for community health. In many studies, besides co-infection with COVID-19, the co-dynamics of TB with HIV, diabetes, smoking, etc. was considered

TB progresses through two main mechanisms: primary infection, which occurs when the disease develops after the initial infection; and endogenous reactivation, which happens when the disease emerges many years after the initial infection [24]. In cases of primary infection, progressive TB can either arise as a continuation of the initial infection or as an endogenous reactivation of a latent focus. The prolonged latency period associated with TB infection creates additional uncertainty about when the disease may become active. As a result of endogenous reactivation, the disease transitions from the latent to the infectious compartment.

Individuals who have been previously infected with TB and are in a latent state could become infected again through a process known as exogenous reinfection, where they contract the disease from another infectious individual [25]. This is particularly common in individuals with compromised immune systems. In this case, the infection is caused by organisms that are not normally present in the body but that have entered from the environment. Therefore, the two key factors in a tuberculosis model that contribute to new infections are the rates of endogenous reactivation and exogenous reinfection. These terms are crucial for understanding the spread of the disease and its impact on the population.

Moreover, in mathematical models, the time lag or delay is a crucial factor that determines the duration of the latent period and the time taken to identify individuals with active TB and start treatment. Delays in the treatment of latent TB can arise due to a variety of factors related to the patient's clinical and demographic characteristics, as well as the

healthcare system. In order to ensure timely diagnosis and treatment of active TB, both the healthcare system and the patient must play a role in identifying and managing the disease. The healthcare system should develop effective case finding strategies, to reduce delays in the diagnosis of active TB, while patients should be aware of the symptoms of TB and seek medical attention promptly if they suspect they might have the disease. A model accounting for treatment was proposed in [26]. The effects of treatment were also discussed in [27].

We follow models of endogenous reactivation and exogenous reinfection [28] and treatment [29], and their fractional-order counterparts [30,31], respectively. Commonly, mathematical models utilize integer-order derivatives to describe the dynamics of systems. However, these conventional models have certain drawbacks, as they do not take into account the learning process and memory effects. On the other hand, fractional models are more suitable, as they can accurately capture these factors and produce more realistic outcomes. This is because fractional derivatives enable models to account for non-local interactions and long-range memory effects that are often present in natural systems. Therefore, incorporating fractional derivatives into models can provide a better understanding of the real-world phenomena being studied. In recent years, there has been a growing interest in non-integer-order biological systems, which are better suited to natural phenomena compared to integer-order systems, as they can account for the memory and hereditary properties of dynamical systems. Fractional-order models, unlike integer-order models, can capture nonlocal relations in time and space through power-law memory kernels. This is due to the fact that the fractional-order derivative provides a greater degree of freedom and is consistent with the reality of interactions, allowing for an exact expression of nonlinear phenomena. Many biological systems involve long-range space interactions and/or temporal memory, and the presence of both fractional order and time delay in a mathematical model can significantly increase the complexity of the observed behavior.

Not many papers, however, have discussed the question of the proper calibration of the proposed models, especially with real data [32]. In [33,34] we calibrated SIR-type fractional-order epidemiological models with time-dependent parameters, fitted to real COVID-19 data. Here, we adopt a different approach.

Motivated by the aforementioned studies, we enhanced the described models with endogenous reactivation, exogenous reinfection and treatment compartment, equipping them with fractional-order derivatives and a time lag. This is one of the two main novelties of the study. The resulting models are described in the next section. Section 3 covers some basic concepts of the fractional calculus required for the following exposition. Section 4 is dedicated to the solution to the direct problem and a basic analysis. The inverse problem is thoroughly described in Section 5, which is the second main novelty. The numerical computations are given in Section 6, while the last section concludes the paper.

## 2. Problem Formulation

Research on the spread of infectious diseases is a field of study that has been around for a long time and has led to the development of the scientific area known as *mathematical epidemiology*. Mathematical epidemiology is a discipline that creates models to aid in the comprehension of epidemics and the development of strategies for the control of infectious diseases. These models have found broad application in fields such as biology, ecology, and chemistry [35]. They allow us to understand underlying processes and forecast the behavior of an epidemic.

In this section, we first propose a classical integer-order derivative model. As mentioned, to compose the model, we primarily follow [30,31].

### 2.1. Integer-Order Model

The total population considered  $N(t)$  is divided into five compartments, plus one additional: the susceptible class  $S(t)$ , the exposed  $E(t)$ , the infectious  $I(t)$ , the treated  $T(t)$ , and the recovered class  $R(t)$ . Here, we also consider the deceased class  $D(t)$ , which is

composed of only deceased individuals from TB infection. The per capita mortality rate is  $\xi$ , which acts in all compartments. The vital dynamics is complemented by the constant birth rate  $\Lambda$ , which increases those susceptible. The infection spreads via *mass action*, where the effective transmission coefficient is  $\beta$ , and this is modeled with a bilinear incidence rate. A fraction  $c \in (0, 1)$  of the newly contaminated population undergoes rapid infection progression and directly enters the infected class, where they become infectious, i.e., can infect susceptible individuals through contact. The rest of the contaminated join the exposed class, where they are not yet infectious. A new infection may arise in a latent individual due to the latency period with length  $k^{-1}$ , where  $k$  is the endogenous reactivation rate. The portion  $\rho \in (0, 1)$  denotes the share of (exogenous) reinfection from the new infections.

The treatment rate  $h$  describes the rate at which the infected are identified and start treatment. The infectious- and treated-induced mortality rates due to TB disease are  $\sigma_1$  and  $\sigma_2$ , respectively. With  $\delta$ , the incomplete treatment rate is denoted. A portion  $\zeta \in (0, 1)$  of the latter subpopulation reenters the infectious, and the remainder the exposed, classes. The successfully treated individuals join the recovered population at rate  $\phi$ . However, the immunity gained is not lifelong, and the parameter  $\gamma$  represents the immunity wane.

Following this, the integer-order derivative model has the form:

$$\begin{aligned} \dot{S}(t) &= \Lambda - \beta S(t)I(t) - \xi S(t), \\ \dot{E}(t) &= (1 - c)\beta S(t)I(t) - \rho\beta E(t)I(t) - kE(t) - \xi E(t) + (1 - \zeta)\delta T(t) + \gamma\beta I(t)R(t), \\ \dot{I}(t) &= c\beta S(t)I(t) + \rho\beta E(t)I(t) + kE(t) - hI(t) - \sigma_1 I(t) - \xi I(t) + \zeta\delta T(t), \\ \dot{T}(t) &= hI(t) - \phi T(t) - \sigma_2 T(t) - \xi T(t) - \delta T(t), \\ \dot{R}(t) &= \phi T(t) - \xi R(t) - \gamma\beta I(t)R(t), \end{aligned} \tag{1}$$

where  $N(t) = S(t) + E(t) + I(t) + T(t) + R(t)$  is the total population size and the additional compartment

$$\dot{D}(t) = \sigma_1 I(t) + \sigma_2 T(t) \tag{2}$$

designates those deceased only from TB disease.

The model is visually represented in Figure 1.

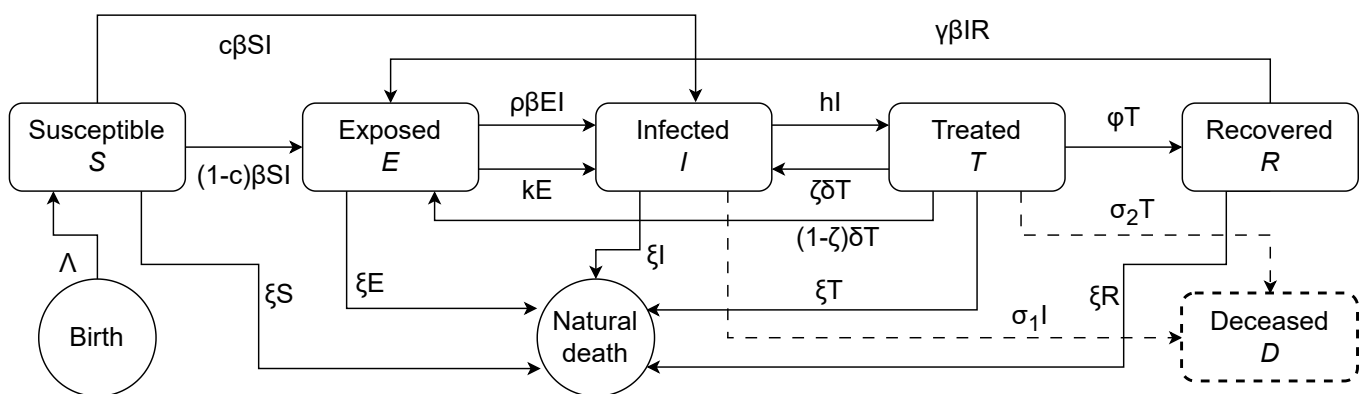


Figure 1. Model Equations (1) and (2).

The model Equation (1) is subjected to non-negative initial conditions

$$S(0) \geq 0, \quad E(0) \geq 0, \quad I(0) \geq 0, \quad T(0) \geq 0, \quad R(0) \geq 0. \tag{3}$$

### 2.2. Fractional-Order Model

Now, we enhance the previous model Equation (1) by introducing two kinds of heritage: fractional order ( $0 < \alpha \leq 1$ ), and discrete time delay  $\tau$ . The inclusion of a time lag accounts for short-term memory, while the use of fractional order accounts for the long-term temporal memory of the system. This modified model is given by the following system:

$$\begin{aligned}
 D^\alpha S(t) &= \Lambda - \beta S(t)I(t) - \zeta S(t), \\
 D^\alpha E(t) &= (1 - c)\beta S(t)I(t) - \rho\beta E(t)I(t) - kE(t) - \zeta E(t) + (1 - \zeta)\delta T(t) + \gamma\beta I(t)R(t), \\
 D^\alpha I(t) &= c\beta S(t)I(t) + \rho\beta E(t)I(t) + kE(t) - hI(t) - \sigma_1 I(t) - \zeta I(t) + \zeta\delta T(t), \\
 D^\alpha T(t) &= hI(t) - \phi T(t) - \sigma_2 T(t) - \zeta T(t) - \delta T(t), \\
 D^\alpha R(t) &= \phi T(t) - \zeta R(t) - \gamma\beta I(t)R(t - \tau),
 \end{aligned}
 \tag{4}$$

where  $D^\alpha$  represents the fractional operator of order  $0 < \alpha \leq 1$ , e.g., of Caputo type. The discrete delay  $\tau$  denotes the time required for the infectious to recover [30], and

$$D^\alpha D(t) = \sigma_1 I(t) + \sigma_2 T(t). \tag{5}$$

Of course, the initial conditions Equation (3) have to be modified accordingly:

$$S(0) \geq 0, \quad E(0) \geq 0, \quad I(0) \geq 0, \quad T(0) \geq 0, \quad R(\theta) \geq 0 \text{ for } -\tau \leq \theta \leq 0. \tag{6}$$

For convenience, we give detailed information of the parameters in Table 1.

**Table 1.** Description of the parameters in model Equations (1) and (4).

Parameter	Description	Typical Values	Reference
$\Lambda$	Birth rate	0.01	[36]
$\zeta$	Natural mortality rate	0.01	[36]
$\beta$	Transmission rate	0.8	Implied
$c$	Portion of “fast” infections	0.5	Implied
$\rho$	Exogenous reinfection rate	0.23	Implied
$k$	Endogenous reactivation rate	0.002	Implied
$\zeta$	Portion of drug defiance treated population	0.3	[31]
$\delta$	Incomplete (failed) treatment rate	0.065	[31]
$\gamma$	Waning immunity rate	0.5	Implied
$h$	Treatment rate	0.15	[31]
$\sigma_1$	Disease-induced mortality rate of infected	0.17	Implied
$\sigma_2$	Disease-induced mortality rate of treated	0.07	Implied
$\phi$	Recovery rate	0.01	[31]

### 2.3. The Direct and Inverse Problems

If the coefficients in Equation (4) are known, obtaining the functions  $S(t), E(t), I(t), T(t), R(t)$  for  $t > 0$  constitutes solving the direct problem. However, in practice, the values of many of the parameters are unknown. They cannot be measures, but are vital for modeling the population, forecasting the future development, and taking adequate measures to control TB disease.

Statistics supply data of the detected infectious people, as well as the deaths from TB. This means that we already know the functions  $I(t_k)$  and  $D(t_k)$  for some time instances  $t_k \in [0, T], k = 1, \dots, K$ . Our problem becomes to find the implied values of the unknown parameters  $\mathbf{p} \equiv \{\beta, c, \rho, k, \gamma, \sigma_1, \sigma_2\}$ , if the following is available:

$$\begin{aligned} I(t_k; \mathbf{p}) &= X_k, \quad k = 1, \dots, K, \\ D(t_k; \mathbf{p}) &= Y_k, \quad k = 1, \dots, K. \end{aligned} \quad (7)$$

The process of determining the value of the parameter  $\mathbf{p}$  is known as an *inverse* problem, which involves modifying the parameter values of a mathematical model to match the observed data. In other words, it is the task of finding the appropriate parameter values that would allow the model to replicate the data that have been collected. This process is often necessary in both real applications and scientific research, particularly when it comes to understanding complex phenomena that cannot be directly observed.

The observations in Equation (7) are called *point* measurements and the model is calibrated via minimizing the following cost functional:

$$\Phi = \Phi(\mathbf{p}) = \sum_{k=1}^K [I(t_k; \mathbf{p}) - X_k]^2 + \sum_{k=1}^K [D(t_k; \mathbf{p}) - Y_k]^2, \quad t \in [0, T]. \quad (8)$$

### 3. Basic Facts Fractional Calculus

Here, we provide some basic notations and definitions, which are required for the following analysis. It is far from a comprehensive review; a much more thorough introduction to fractional calculus can be found f. i. in [37,38].

Hereinafter, we assume  $f \in \mathcal{AC}[0, T]$ , i.e.,  $f$  is absolutely continuous on  $[0, T]$ , and  $\alpha \in [0, 1]$ .

**Definition 1** ((Forward) Riemann–Liouville integral).

$$(J_{0+}^{\alpha} f)(t) := \begin{cases} f(t), & \alpha = 0, \\ \frac{1}{\Gamma(\alpha)} \int_0^t \frac{f(s)}{(t-s)^{1-\alpha}} ds, & 0 < \alpha \leq 1, \end{cases} \quad t \in [0, T],$$

where  $\Gamma$  denotes the Gamma function  $\Gamma(x) := \int_0^{\infty} s^{x-1} e^{-s} ds$  for  $x > 0$ .

**Definition 2** ((Forward) Caputo fractional derivative).

$${}^c D_{0+}^{\alpha} f(t) = \left( J_{0+}^{1-\alpha} \frac{df}{dt} \right)(t) = \frac{1}{\Gamma(1-\alpha)} \int_0^t \frac{1}{(t-s)^{\alpha}} \frac{df}{dt} ds.$$

For monotonicity, we recall the following [37]:

**Lemma 1** (Generalized mean value formula). *Let  $f(t) \in \mathcal{C}[a, b]$  and  $D_{0+}^{\alpha} f(t) \in \mathcal{C}[a, b]$  for  $0 < \alpha \leq 1$ . If*

$$D_{0+}^{\alpha} f(t) \geq 0 \quad \forall t \in (a, b), \text{ then } f(t) \text{ is nondecreasing, } \forall t \in [a, b];$$

$$D_{0+}^{\alpha} f(t) \leq 0 \quad \forall t \in (a, b), \text{ then } f(t) \text{ is nonincreasing, } \forall t \in [a, b].$$

## 4. Solution to the Direct Problem

In this section, a number of important properties of the continuous model are given in Equations (4)–(6). Then, the numerical approach to solving the latter is discussed.

### 4.1. Continuous Solution Properties

**Proposition 1** (Existence, positivity, and boundedness). *The solution to model Equations (4) and (6) is unique, nonnegative, and bounded for every  $(S(0), E(0), I(0), T(0), R(0)) \in \mathbb{R}_+^5$  and  $t > 0$ .*

Proposition 1 follows from the results in [39] and Lemma 1.

To find the equilibria states of the model Equation (4), one is required to solve the system

$$D^\alpha S(t) = D^\alpha E(t) = D^\alpha I(t) = D^\alpha T(t) = D^\alpha R(t) = 0.$$

**Proposition 2** (Equilibria states). *Model Equation (4) exhibits a disease-free equilibrium (DFE) point at*

$$\mathcal{E}_0 = \left( \frac{\Lambda}{\zeta}, 0, 0, 0, 0 \right) \tag{9}$$

*and endemic equilibrium (EE) point at*

$$\mathcal{E}_1 = (S^*, E^*, I^*, T^*, R^*), \tag{10}$$

where

$$\begin{cases} S^* = \frac{\Lambda}{\zeta + \beta I^*}, \\ E^* = \frac{m_2 \zeta - \Lambda \beta c + \beta m_2 I^* - \delta \zeta \zeta - \beta \delta \zeta I^*}{(\zeta + \beta I^*)(k + \beta \rho I^*)} I^*, \\ T^* = \frac{h}{m_3} I^*, \\ R^* = \frac{\phi h}{m_3(\zeta + \beta \gamma I^*)} I^*, \end{cases} \tag{11}$$

$m_{1,2,3}$  are defined in Equation (13) and  $I^*$  is the real positive root to the cubic equation

$$\tilde{a}(I^*)^3 + \tilde{b}(I^*)^2 + \tilde{c}I^* + \tilde{d} = 0. \tag{12}$$

The coefficients  $\tilde{a}$ ,  $\tilde{b}$ ,  $\tilde{c}$ , and  $\tilde{d}$  are given in Appendix A.

In the field of mathematical epidemiology, the basic reproduction number  $\mathcal{R}_0$  is a concept that carries significant importance [40]. It can be described as a measure of the contagiousness of a specific disease [41]. The study of infectious disease modeling has shown that the basic reproduction number plays a key role in predicting the dynamics of an epidemic. It serves as a threshold for the behavior of the epidemic, indicating an abrupt change in behavior depending on whether the number is greater than one or less than one. This phenomenon is known as threshold behavior, and it has been extensively studied [42].

The next generation method [42] allows us to compute the basic reproduction number for the model Equation (4):

$$F = \begin{pmatrix} 0 & (1-c)\beta\frac{\Lambda}{\zeta} & 0 \\ 0 & c\beta\frac{\Lambda}{\zeta} & 0 \\ 0 & 0 & 0 \end{pmatrix}, \quad V = \begin{pmatrix} m_1 & 0 & -(1-\zeta)\delta \\ -k & m_2 & -\zeta\delta \\ 0 & -h & m_3 \end{pmatrix},$$

where

$$m_1 = k + \zeta, \quad m_2 = h + \sigma_1 + \zeta, \quad m_3 = \phi + \sigma_2 + \zeta + \delta \tag{13}$$

and eventually

**Proposition 3** (Basic reproduction number).

$$\mathcal{R}_0 = \frac{\Lambda}{\zeta} \cdot \frac{\beta k m_3 + \beta c m_1 m_3 - \beta c k m_3}{\delta \zeta h k - \delta h k - \delta \zeta h m_1 + m_1 m_2 m_3}. \tag{14}$$

To put this in a more technical manner, the basic reproduction number  $\mathcal{R}_0$  quantifies the average number of new infections that can be caused by a single infected individual during their infectious period in a fully susceptible population. In simpler terms, it measures the contagiousness of a disease and its potential to cause an epidemic. When  $\mathcal{R}_0 < 1$ , this means that each infected individual, on average, infects fewer than one susceptible individual, indicating that the disease is likely to die out. However, if  $\mathcal{R}_0 > 1$ , this implies that each infected individual will infect more than one susceptible individual, and the disease is expected to continue spreading among the population. The basic reproduction number is a crucial parameter in epidemiological models, as it helps in predicting the trajectory of an outbreak and designing appropriate control measures.

Before further studying equilibria states, we will measure the sensitivity of  $\mathcal{R}_0$  to the parameters involved in it. Basically, the sensitivity analysis reveals how important is each of the parameters in the model. It quantifies the impact a particular parameter has on a variable. The sensitivity of the basic reproduction number with respect to a parameter is the proportion of the relative change in  $\mathcal{R}_0$  to relative change in  $p$ . Assuming  $\mathcal{R}_0$  is a differentiable function of the parameters, then the sensitivity indices can be written by means of the partial derivatives:

$$S_p^{\mathcal{R}_0} = \frac{p}{\mathcal{R}_0} \cdot \frac{\partial \mathcal{R}_0}{\partial p}.$$

In particular,

$$\begin{aligned} S_{\Lambda}^{\mathcal{R}_0} &= 1 > 0 & S_{\xi}^{\mathcal{R}_0} &< 0 \\ S_{\beta}^{\mathcal{R}_0} &= 1 > 0 & S_h^{\mathcal{R}_0} &< 0 \\ S_c^{\mathcal{R}_0} &= \frac{c\zeta}{k + c\zeta} > 0 & S_{\sigma_1}^{\mathcal{R}_0} &< 0 \\ S_k^{\mathcal{R}_0} &> 0 & S_{\sigma_2}^{\mathcal{R}_0} &< 0 \\ S_{\zeta}^{\mathcal{R}_0} &> 0 & S_{\phi}^{\mathcal{R}_0} &< 0 \\ S_{\delta}^{\mathcal{R}_0} &> 0 & & \end{aligned}$$

Obviously,  $\Lambda$  and  $\beta$  are directly proportional to  $\mathcal{R}_0$ , in the sense that one unit change in them will cause exactly one unit change in  $\mathcal{R}_0$ . The parameters  $c$ ,  $k$ ,  $\zeta$  and  $\delta$  are also directly proportional to the basic reproduction number, while the parameters  $\xi$ ,  $h$ ,  $\sigma_1$ ,  $\sigma_2$  and  $\phi$  are inversely proportional to  $\mathcal{R}_0$ . The latter does not depend on  $\rho$  or  $\gamma$ . A respective increase or decrease in the parameters leads to minimizing or maximizing the endemic nature of TB, which could be used in an optimal control framework.

Now, we continue with an equilibrium study.

**Theorem 1** (Equilibrium stability). *The DFE  $\mathcal{E}_0$  Equation (9) of model Equation (4) is locally asymptotically stable if*

$$\beta < \frac{\xi}{\Lambda} \min \left\{ \frac{m_1 + m_2 + m_3}{c}, \frac{m_1 m_2 + m_1 m_3 + m_2 m_3 - \delta h \zeta}{k + cm_1 + cm_3 - ck}, -\frac{b + \Re(\sqrt{b^2 - 4ac})}{2a} \right\} \text{ and } \mathcal{R}_0 < 1$$

and unstable if  $\mathcal{R}_0 > 1$ , where

$$a = c(k + cm_1 + cm_3 - ck),$$

$$b = km_3 - (m_1 + m_2 + m_3)(k + cm_1 + cm_3 - ck) - c(m_1 m_2 + m_2 m_3 - \delta h \zeta + km_3),$$

$$c = (m_1 + m_2 + m_3)(m_1 m_2 + m_1 m_3 + m_2 m_3 - \delta h \zeta) + \delta hk - m_1 m_2 m_3 - \delta hk \zeta + \delta h m_1 \zeta.$$

**Proof.** The characteristic matrix, evaluated at  $\mathcal{E}_0$ , is

$$J(\mathcal{E}_0) = \begin{pmatrix} -\zeta & 0 & -\frac{\Lambda}{\zeta}\beta & 0 & 0 \\ 0 & -m_1 & (1-c)\frac{\Lambda}{\zeta}\beta & (1-\zeta)\delta & 0 \\ 0 & k & c\frac{\Lambda}{\zeta}\beta - m_2 & \zeta\delta & 0 \\ 0 & 0 & h & -m_3 & 0 \\ 0 & 0 & 0 & \phi & -\zeta \end{pmatrix}.$$

Taking into consideration both  $-\zeta$ , the remaining part of the characteristic equation at  $\mathcal{E}_0$  is

$$P(\lambda) = \lambda^3 + a_2\lambda^2 + a_1\lambda + a_0,$$

where

$$\begin{aligned} a_2 &= m_1 + m_2 + m_3 - c\frac{\Lambda}{\zeta}\beta, \\ a_1 &= m_1m_2 + m_1m_3 + m_2m_3 - \delta h\zeta - \frac{\Lambda}{\zeta}\beta(k + cm_3 + cm_1 - ck), \\ a_0 &= m_1m_2m_3 - \delta hk - \delta hm_1\zeta + \delta h k\zeta - \frac{\Lambda}{\zeta}\beta(km_3 + cm_1m_3 - ck m_3). \end{aligned}$$

The Routh–Hurwitz criteria requires

$$a_2 > 0, \quad a_1 > 0, \quad a_0 > 0, \quad a_2a_1 - a_0 > 0 \quad (15)$$

so that all roots of  $P(\lambda)$  lie in the open left half-plane.

The first condition in Equation (15) reduces to

$$\frac{\Lambda}{\zeta}\beta < \frac{m_1 + m_2 + m_3}{c},$$

the second condition reduces to

$$\frac{\Lambda}{\zeta}\beta < \underbrace{\frac{m_1m_2 + m_1m_3 + m_2m_3 - \delta h\zeta}{k + cm_1 + cm_3 - ck}}_{\mathfrak{B}},$$

and  $a_0 > 0$  is equivalent to  $\mathcal{R}_0 < 1$ .

Reordering the terms of  $a_2a_1 - a_0$  yields  $a\left(\frac{\Lambda}{\zeta}\beta\right)^2 + b\left(\frac{\Lambda}{\zeta}\beta\right) + c$ . From  $m_1 > k$  it is obvious that  $a > 0$ , i.e., the parabola is upward (convex); therefore,  $\frac{\Lambda}{\zeta}\beta$  must be less than the lower root and more than the greater root, if any. However, the parabola vertex is

$$v = -\frac{b}{2a} = \underbrace{\frac{(1-c)km_1 + (1-c)km_2 + c(m_1^2 + m_2^2 + \delta h\zeta)}{2c(k + cm_1 + cm_3 - ck)}}_{>0} + \mathfrak{B},$$

which means the right branch surely violates the second condition. Thus,  $\frac{\Lambda}{\zeta}\beta$  must be less than the lower root, if it exists.  $\square$

#### 4.2. Numerical Solution

This subsection is dedicated to presenting the numerical procedure required to solve the direct problem Equations (4)–(6). We employ the following equidistant grid:

$$\bar{\omega}_{\Delta t}^{\text{dir}} = \{t_0 = 0, t_j = j\Delta t, t_J = T\} \text{ for } j = 1, \dots, J - 1 \tag{16}$$

with a constant step size  $\Delta t$ .

The fractional-order model Equations (4) and (5) are solved with  $\bar{\omega}_{\Delta t}^{\text{dir}}$  Equation (16). Now, we consider a modified Adams–Bashforth–Moulton (fractional Adams) scheme to deal with the delay. The system Equation (4) is written as

$${}^c D_0^\alpha \mathbf{y} = \mathbf{F}(t, \mathbf{y}(t), \mathbf{y}(t - \tau)),$$

which is identical to the Volterra integral equation

$$\mathbf{y}(t) = \mathbf{y}_0 + \frac{1}{\Gamma(\alpha)} \int_0^t \frac{\mathbf{F}(s, \mathbf{y}(s), \mathbf{y}(s - \tau))}{(t - s)^{1-\alpha}} ds,$$

and we solve it by means of Algorithm 1. This is a single-step method, i.e., only the initial condition Equation (6) is needed to begin with.

---

**Algorithm 1** Fractional Adams method [43]

---

**for**  $j = 0, \dots, J - 1$  **do**

Let  $t := t_j, \hat{t} := t_{j+1}, \check{\mathbf{y}} := \mathbf{y}(t - \tau), \mathbf{y} := \mathbf{y}(t), \hat{\mathbf{y}} := \mathbf{y}(\hat{t})$ . Then  $\hat{\mathbf{y}}$  is calculated as

$$\begin{aligned} \hat{\mathbf{y}}^{\text{pred}} &= \mathbf{y}_0 + \frac{1}{\Gamma(\alpha)} \sum_{i=0}^j b_{i,j+1} \mathbf{F}(t, \mathbf{y}, \check{\mathbf{y}}), \\ \hat{\mathbf{y}} &= \mathbf{y}_0 + \frac{1}{\Gamma(\alpha)} \left( \sum_{i=0}^j a_{i,j+1} \mathbf{F}(t, \mathbf{y}, \check{\mathbf{y}}) + a_{i+1,j+1} \mathbf{F}(\hat{t}, \hat{\mathbf{y}}^{\text{pred}}, \mathbf{y}(\hat{t} - \tau)) \right), \end{aligned}$$

where

$$a_{i,j+1} = \frac{\Delta t^\alpha}{\alpha(\alpha + 1)} \begin{cases} j^{\alpha+1} - (j - \alpha)(j + 1)^\alpha, & i = 0, \\ (j - i + 2)^{\alpha+1} - 2(j - i + 1)^{\alpha+1} + (j - i)^{\alpha+1}, & 1 \leq i \leq j, \\ 1, & i = j + 1, \end{cases}$$

$$b_{i,j+1} = \frac{\Delta t^\alpha}{\alpha} ((j - i + 1)^\alpha - (j - i)^\alpha), \quad 0 \leq i \leq j.$$

**end for**

---

Although basic, this method is unconditionally stable and computationally efficient. Different procedures could be used.

#### 5. Numerical Solution to the Inverse Problem

Here, we present the numerical approach to solving the inverse problem Equations (4)–(7). The new temporal grid  $\bar{\omega}_{\Delta t}^{\text{inv}}$  Equation (17) is as follows:

$$\bar{\omega}_{\Delta t}^{\text{inv}} = \{t^0 = t_0 = 0, t^i = t_{m_i}, t_1 = t_J = T\} \text{ for } i = 1, \dots, I - 1 \text{ and } m_i = j \text{ for some } i \leq j. \tag{17}$$

The nodes  $t^i$  designate each point in which a measurement Equation (7) is available. Unfortunately, in general, data are collected on an annual basis, in contrast to COVID-19

statistics, for example, where the data are updated daily. Thus,  $t^i$  are the moments at the end of every year, where the annual data are reported [36].

The point of minimum  $\check{\mathbf{p}}$  of the functional  $\Phi(\mathbf{p})$  Equation (8) is called a *nonlinear least squares estimator (LSE)*. To find it, or to minimize  $\Phi(\mathbf{p})$ , we use the Levenberg–Marquardt algorithm.

To assess the performance of the estimator  $\check{\mathbf{p}}$ , we utilize various metrics to validate its convergence. These metrics are divided into two categories: those associated with the estimator itself, and those that gauge the goodness of fit.

The norm of the step  $\delta\mathbf{p}_k$  is the first metric used to measure the difference between two consecutive iterations of the minimizer  $\mathbf{p}^k$  and  $\mathbf{p}_{k+1}$ :

$$\delta\mathbf{p}_k := \|\Delta\mathbf{p}_k\| = \|\mathbf{p}_{k+1} - \mathbf{p}_k\|.$$

The second metric is the relative change in the cost function  $\delta\Phi_k$ , which is defined as follows:

$$\delta\Phi_k := \frac{|\Delta\Phi_k|}{1 + |\Phi(\mathbf{p}_k)|},$$

where  $\Delta\Phi_k := \Phi(\mathbf{p}_{k+1}) - \Phi(\mathbf{p}_k)$  and  $\Phi(\mathbf{p}_k)$  is the cost function at iteration  $k$ .

To ensure that the iterative procedure for obtaining  $\Phi(\mathbf{p})$  is reliable, it is necessary to have an appropriate stopping criterion. One such criterion is expressed as

$$\min\{\delta\mathbf{p}_k, \delta\Phi_k\} < \varepsilon, \tag{18}$$

Here,  $\varepsilon$  is a tolerance value set by the user. If the condition in Equation (18) is satisfied, the iterative procedure terminates at the  $(k + 1)^{\text{th}}$  iteration, and the estimated value of the nonlinear LSE is returned as  $\check{\mathbf{p}} := \mathbf{p}_{k+1}$ .

Various metrics are used to validate the convergence of the estimator  $\check{\mathbf{p}}$ , including the *norm of the step*  $\delta\mathbf{p}_k$ , which measures the difference between the previous and current iterations of the estimator. The *relative change in the cost function*  $\delta\Phi_k$  is another metric that measures the degree of convergence of the algorithm. The *first-order optimality measure* is also used to evaluate how closely the estimator  $\check{\mathbf{p}}$  approximates the true minimum of Equation (8). This measure is calculated as the infinity norm of the gradient of the objective function  $\Phi$  evaluated at LSE, which corresponds to the maximum absolute value of the partial derivatives of  $\Phi$  with respect to the parameter vector  $\mathbf{p}$ :

$$\|\nabla\Phi(\check{\mathbf{p}})\|_\infty = \max_{i=1,7} \left| \frac{\partial\Phi}{\partial p^i}(\check{\mathbf{p}}) \right|.$$

Furthermore, to assess the performance of the model in fitting the data, we calculate several metrics after obtaining the nonlinear LSE. These metrics are associated with the goodness of fit and include the variance of the residuals, root mean squared error (RMSE), and coefficient of determination:

$$\tilde{\sigma}^2 = \frac{\Phi(\check{\mathbf{p}})}{K}, \quad \hat{\sigma} = \sqrt{\frac{\Phi(\check{\mathbf{p}})}{K-3}}, \quad R^2 = 1 - \frac{\Phi(\check{\mathbf{p}})}{\sum_{k=1}^K \left( \sum_{\Psi \in \{X,Y\}} (\Psi(t_k) - \bar{\Psi})^2 \right)},$$

The variance of the residuals and RMSE are metrics where lower values indicate a better model fit to the data. On the other hand, the coefficient of determination assesses how well the model fits the data mean and is a metric where higher values indicate a better model fit, but not greater than one. The mean value of the experimental data is denoted by  $\bar{\Psi} = \frac{\sum_{k=1}^K \Psi(t_k)}{K}$ .

If the residuals  $(\Xi(t_k; \mathbf{p}) - \Psi_k)$ ,  $\Xi \in \{I, D\}$  are distributed normally or the number of observations  $K$  is large enough, it is possible to estimate the covariance matrix of the

nonlinear LSE  $\check{\mathbf{p}}$  using Equation (19). This equation uses the sensitivity or Jacobian matrix, denoted as  $J(\check{\mathbf{p}})$ , which is calculated at the value of  $\check{\mathbf{p}}$ :

$$\Sigma = \frac{\hat{\sigma}^2}{J^\top(\check{\mathbf{p}})J(\check{\mathbf{p}})}, \quad (19)$$

where

$$J(\check{\mathbf{p}}) = \left( \frac{\partial I(\check{\mathbf{p}})}{\partial \mathbf{p}}, \frac{\partial D(\check{\mathbf{p}})}{\partial \mathbf{p}} \right)^\top.$$

The sensitivity matrix  $J(\mathbf{p})$  indicates how much the values of  $\Psi(t_k; \mathbf{p})$  change with variations in  $\mathbf{p}$ . A sensitivity analysis provides insights into the importance of the measurements for parameter estimation [44]. The covariance matrix in Equation (19) is used to compute the *standard error (SE)*, which is related to the accuracy of the nonlinear LSE  $\check{\mathbf{p}}$  in the parameter recovery. The standard error is defined as follows:

$$\widehat{SE} = \sqrt{\text{diag}(\Sigma)}. \quad (20)$$

## 6. Computational Experiments

In this section, we provide a variety of computational simulations, implemented in MATLAB<sup>®</sup>, to test the suggested approach. First, we solve the direct problem, and the solution to the inverse problem readily follows. We conclude the section with an experiment with real data.

The inverse problem is solved in a synthetic data framework. This means that the values of the parameters  $\mathbf{p}$  are set, and then the direct problem is solved with these parameters. Later, this solution is used to generate the observations Equation (7). Next, the inverse problem is solved with these measurements. The advantage of this is simple, the *implied* values of  $\mathbf{p}$  can be compared with the true ones, which are a priori known in this setting.

In reality, however, these values  $\mathbf{p}$  are unknown, so we need a different approach. The true values of the parameters cannot be assessed, but this is not the case with the implied functions  $I(t)$  and  $D(t)$ ; i.e., the solution to the direct problem with the derived parameter values can be compared to the observed values. For that purpose, the residual measure is introduced later.

### 6.1. Direct Problem

Let us begin by setting  $\Lambda = \zeta = 0.01$ ,  $\zeta = 0.3$ ,  $\delta = 0.05$ ,  $h = 0.15$ ,  $\phi = 0.1$ . Then  $\mathbf{p} \equiv \{\beta, c, \rho, k, \gamma, \sigma_1, \sigma_2\} = \{0.4, 0.5, 0.23, 0.002, 0.5, 0.17, 0.07\}$ . Let  $\tau = 0.7$  be the delay and the fractional order  $\alpha = 0.9$ . A population of 2000 people is considered, and  $S(0) = 1770$ ,  $E(0) = 200$ ,  $I(0) = 30$  and  $T(0) = R(0) = D(0) = 0$ . The considered time period is 200 years, in order for the system to approach the equilibrium state. When  $\beta = 0.4$  is low and  $\mathcal{R}_0 = 0.7374 < 1$ , then there is no epidemic (Figure 2). On the contrary, for  $\beta = 0.8$  and  $\mathcal{R}_0 = 1.4749 > 1$ , the disease persists in the society (Figure 3).

TB disease dynamics:  $\beta=0.4$  and  $R_0=0.7374$

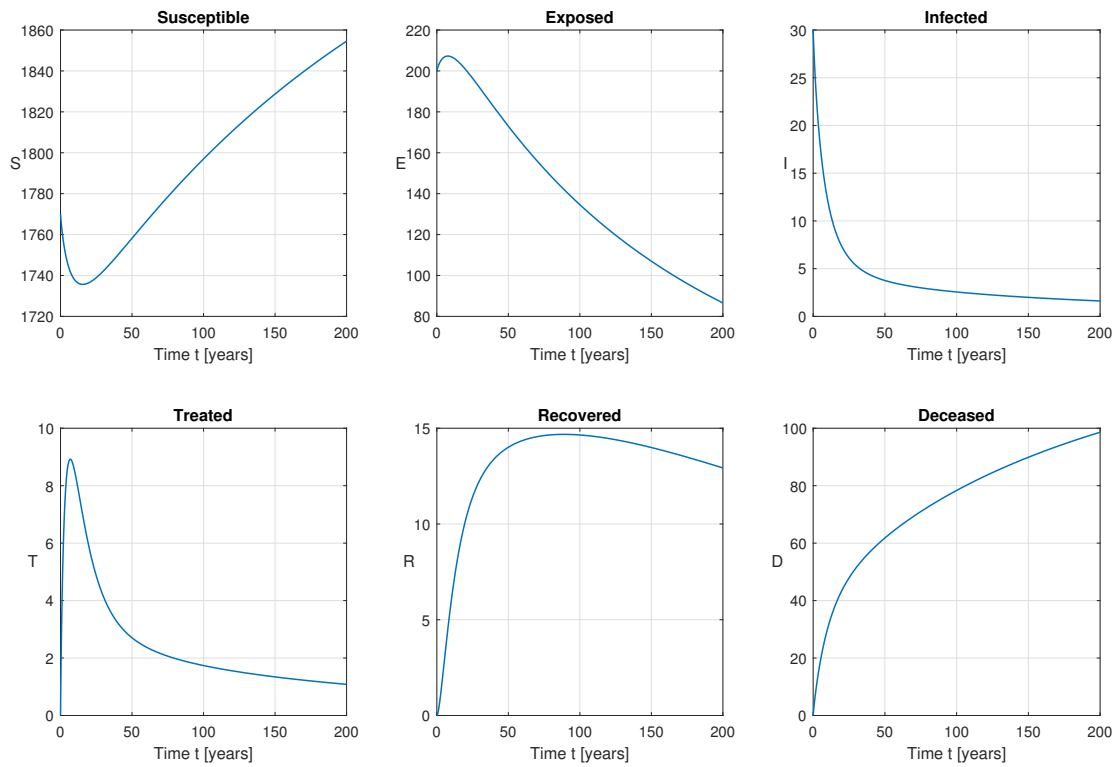


Figure 2. The epidemic dynamics for  $\beta = 0.4$  and  $R_0 = 0.7374 < 1$ .

TB disease dynamics:  $\beta=0.8$  and  $R_0=1.4749$

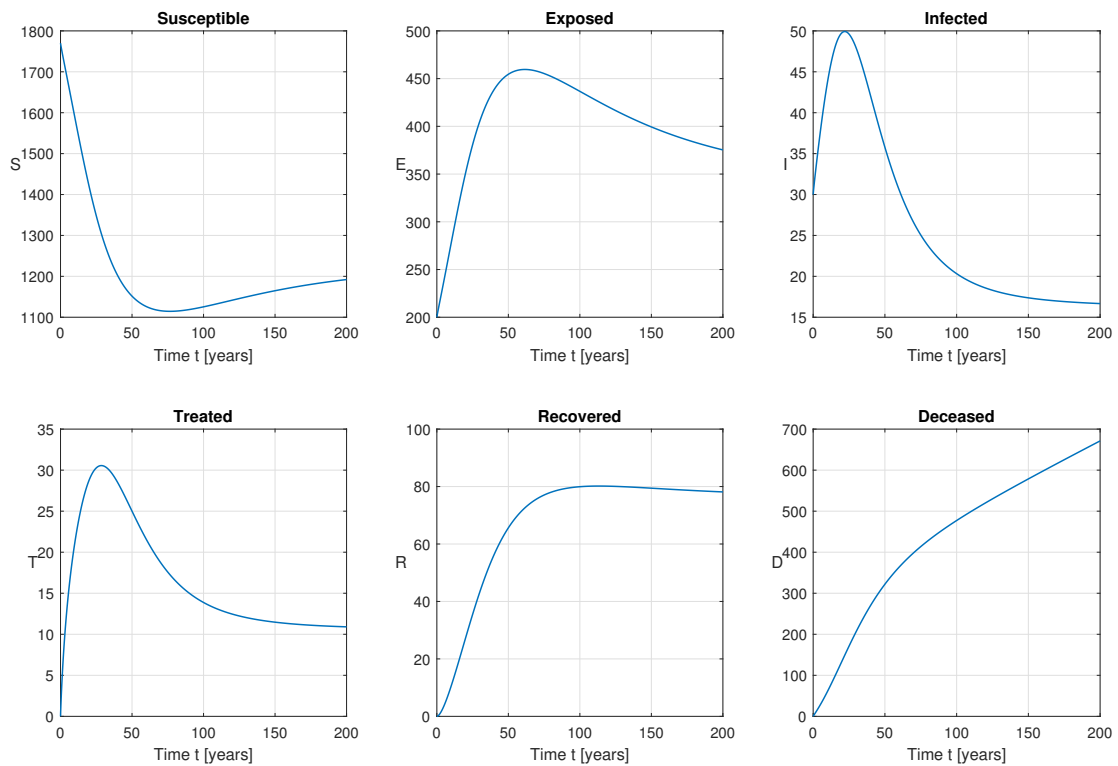


Figure 3. The epidemic dynamics for  $\beta = 0.8$  and  $R_0 = 1.4749 > 1$ .

### 6.2. Inverse Problem

Now, we solve the inverse problem Equations (4)–(7). Let  $\beta = 0.8$  and the regarded period in  $T = 20$  years. All the parameters stay the same as in the direct problem setting, except that  $p$  are not known. However, Equation (7) are provided for each year. The initial approximations of the parameters are  $p_0 = \{0.9, 0.6, 0.3, 0.005, 0.6, 0.2, 0.1\}$ .

The experiment with exact observations is plotted in Figure 4, while the results are given in Table 2.

Identified TB dynamics: implied  $\beta=0.75715$  and  $R_0=1.57$

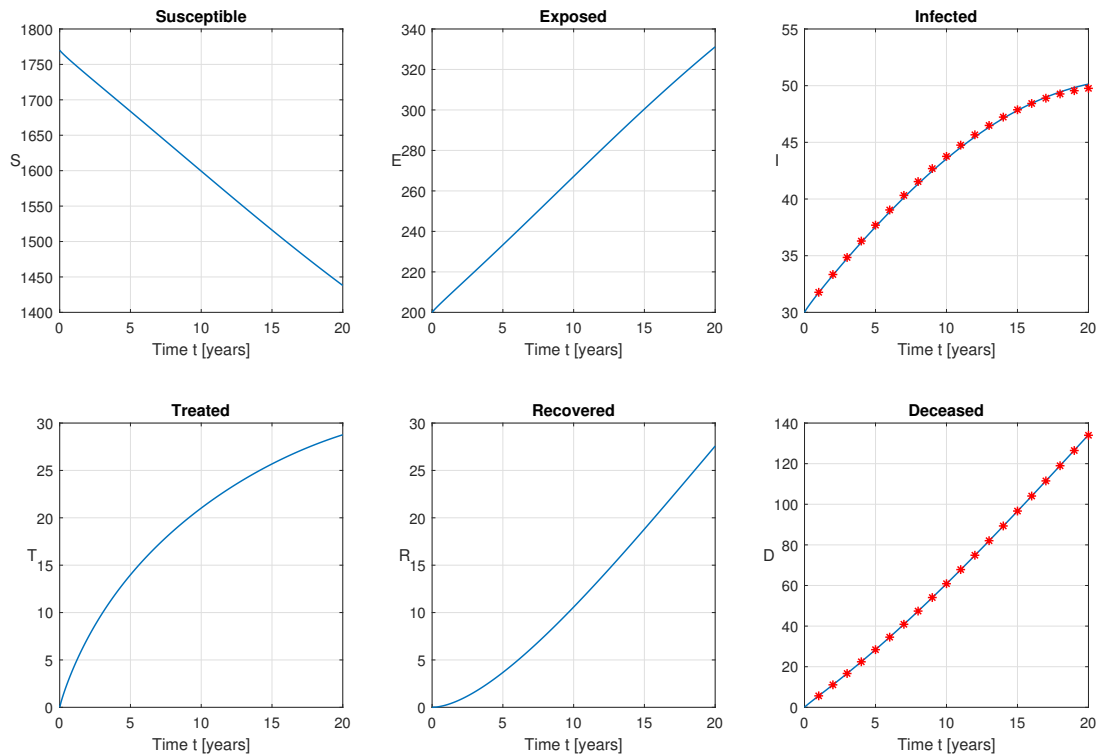


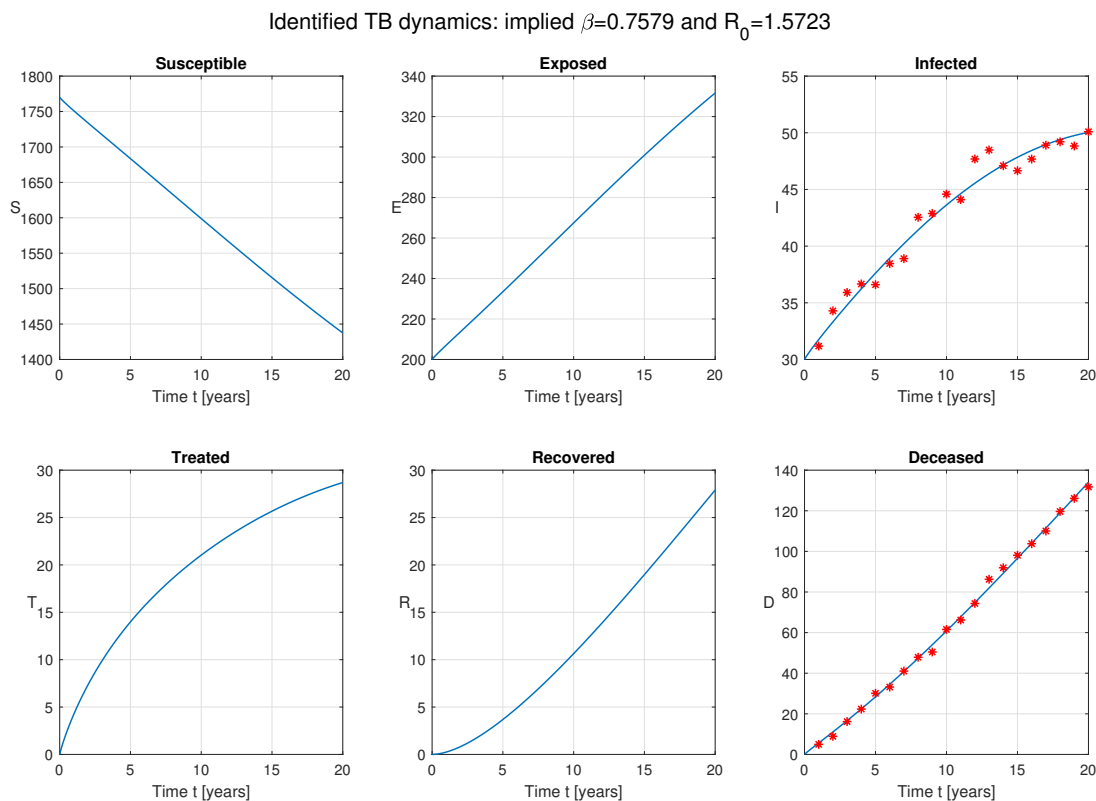
Figure 4. The identified epidemic dynamics for  $\beta = 0.8$  and exact measurements.

Table 2. Parameter  $p$  recovery from exact measurements.

Parameter	$p_0^i$	$p^i$	$\check{p}^i$	$ p^i - \check{p}^i $	$\frac{ p^i - \check{p}^i }{p^i}$	$\widehat{SE}$
$\beta$	0.9	0.8	0.7571	0.0429	0.0536	$1.7565 \times 10^{-4}$
$c$	0.6	0.5	0.5065	0.0065	0.0130	$1.2582 \times 10^{-4}$
$\rho$	0.3	0.23	0.2414	0.0114	0.0497	$8.3171 \times 10^{-4}$
$k$	0.005	0.002	0.0041	0.0021	1.0699	$1.2502 \times 10^{-5}$
$\gamma$	0.6	0.5	0.3334	0.1666	0.3333	0.8049
$\sigma_1$	0.2	0.17	0.1704	$3.7077 \times 10^{-4}$	0.0022	$1.1758 \times 10^{-4}$
$\sigma_2$	0.1	0.07	0.0706	$6.3291 \times 10^{-4}$	0.0090	$3.5894 \times 10^{-4}$

The recovered  $\mathcal{R}_0 = 1.5700$ . It can be observed that the parameters were accurately recovered with small absolute and relative errors.

Next, we perform a test with perturbed measurements. In reality, sometimes the statistics are inexact, due to a number of reasons, thus such an experiment is meaningful. In order to simulate the perturbation, we introduce Gaussian noise to the observations Equation (7). This means that we are 95% confident that any individual measurement’s bias will not exceed 5%. We conducted this test with such a high level of noise, in order to confirm the algorithm’s robustness. The results are displayed in Figure 5 and Table 3.



**Figure 5.** The identified epidemic dynamics for  $\beta = 0.8$  and perturbed measurements.

**Table 3.** Parameter  $p$  recovery from perturbed measurements.

Parameter	$p_0^i$	$p^i$	$\check{p}^i$	$ p^i - \check{p}^i $	$\frac{ p^i - \check{p}^i }{p^i}$	$\widehat{SE}$
$\beta$	0.9	0.8	0.7579	0.0421	0.0526	0.0019
$c$	0.6	0.5	0.5093	0.0093	0.0186	0.0014
$\rho$	0.3	0.23	0.2217	0.0083	0.0360	0.0090
$k$	0.005	0.002	0.0040	0.0020	1.0197	$1.3516 \times 10^{-4}$
$\gamma$	0.6	0.5	0.2146	0.2854	0.5708	9.0682
$\sigma_1$	0.2	0.17	0.1698	$1.6755 \times 10^{-4}$	$9.8561 \times 10^{-4}$	0.0013
$\sigma_2$	0.1	0.07	0.0712	0.0012	0.0174	0.0039

The recovered  $\mathcal{R}_0 = 1.5723$ . The errors were slightly higher but still acceptable. The relative errors (REs) in parameters and functions are further defined as

$$RE_p := \frac{\|\check{p} - \check{p}^{pert}\|_\infty}{\|\check{p}\|_\infty},$$

$$RE_\Xi := \frac{\|\Xi(t; \check{p}) - \Xi(t; \check{p}^{pert})\|_\infty}{\|\Xi(t; \check{p})\|_\infty},$$

where  $\Xi(t; p)$  are the implied solutions for  $\Xi \in \{S, E, I, T, R, D\}$  using  $p$ , and  $\check{p}^{pert}$  is the nonlinear LSE, obtained with the perturbed data.

In our case,  $RE_p = 0.1569$  and  $RE_\Xi = \{0.0004, 0.0014, 0.0021, 0.0024, 0.0121, 0.0008\}$  for  $\Xi \in \{S, E, I, T, R, D\}$ . The relative errors are small, which again implies the advantages of the algorithm.

The gof metric for both cases are given in Table 4. For very little computational effort, the algorithm achieved a sufficient accuracy.

**Table 4.** Goodness-of-fit metrics.

Noise	$\ \nabla\Phi(\check{\mathbf{p}})\ _\infty$	Iter	$\delta\mathbf{p}_k$	$\Phi(\check{\mathbf{p}})$	$\hat{\sigma}^2$	$\hat{\sigma}$	$R^2$
0%	$2.49 \times 10^{-5}$	4	0.272652	$1.75098 \times 10^{-7}$	$8.7549 \times 10^{-9}$	$1.0149 \times 10^{-4}$	$1-2.2158 \times 10^{-5}$
5%	$6.95 \times 10^{-5}$	4	0.407747	$2.05108 \times 10^{-5}$	$1.0255 \times 10^{-6}$	0.0011	0.9974

### 6.3. Calibration to Real Data

Here, we fit the model to real data [36]. We chose Pakistan for two reasons: it is one of the countries most influenced by TB in the world, and the results could be compared to [29,31]. We considered the period 2000–2019, due to the data availability. As discussed, the statistics for infectious and those deceased were presented on an annual basis.

To obtain the measurement for  $I(t_k)$ , we multiplied the incidence rate by the population in the respective year. Since both the birth and mortality rates were high, it was important to do so, otherwise we would have arrived at a flat curve. Considering the deceased from TB, we accumulated the deaths during the years, to obtain the measurement for  $D(t_k)$ ,  $k = 1, \dots, K$ ,  $K = 20$ .

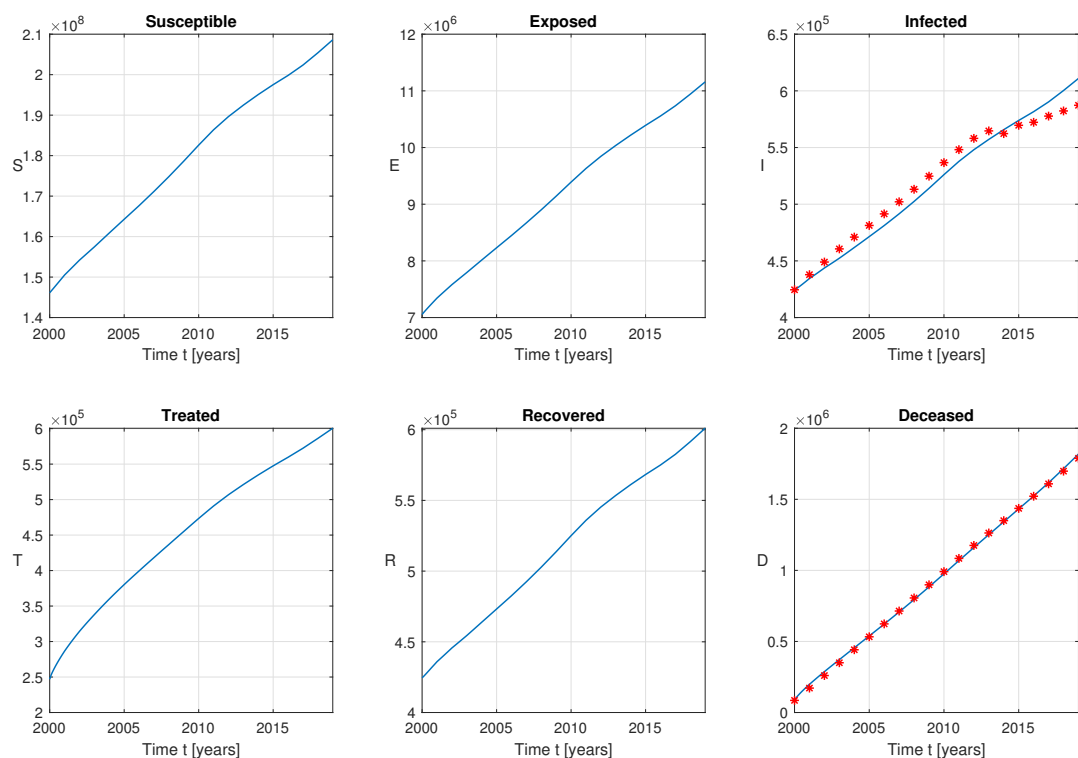
We kept the same settings, except that  $\delta = 0.065$  and  $\phi = 0.01$ . To measure the gof, we used the residuals

$$R(\mathbf{p}) = \|I(\mathbf{p}) - X\|_2 + \|D(\mathbf{p}) - Y\|_2. \quad (21)$$

It also helped us to determine the optimal fractional order. Empirically, we deduced that  $\alpha = 0.8$ , since this yielded the smallest residual norm Equation (21)  $R(\mathbf{p}) = 1.9619 \times 10^{-7}$ . The derived basic reproduction number was  $\mathcal{R}_0 = 1.1908$ , and the implied parameters were  $\check{\mathbf{p}} = \{0.6661, 0.4456, 0.2259, 0.0036, 0.4215, 0.2071, 0.0452\}$ , which are close to those in [31].

Finally, the calibration is visualized in Figure 6, and the gof quantities are given in Table 5.

Identified TB dynamics in Pakistan: implied  $\beta=0.66614$  and  $R_0=1.1908$

**Figure 6.** The identified epidemic dynamics for Pakistan.

**Table 5.** Goodness-of-fit metrics for the real-world data fit

$\ \nabla\Phi(\check{\mathbf{p}})\ _\infty$	Iter	$\delta\mathbf{p}_k$	$\Phi(\check{\mathbf{p}})$	$\tilde{\sigma}^2$	$\hat{\sigma}$	$R^2$
$4.5 \times 10^{-7}$	5	0.086884	$1.9619 \times 10^{-7}$	$9.8095 \times 10^{-9}$	$1.0743 \times 10^{-4}$	0.9981

The high values of  $\mathcal{R}_0 = 1.1908$  and  $\beta = 0.6661$  unequivocally demonstrate that TB has not disappeared in Pakistan.

#### 6.4. Discussion

In this study, we constructed model Equations (4)–(6) to account for endogenous reactivation and exogenous reinfection, incomplete treatment, slow and fast contagion, as well as short and long memory effects, all of which are typical of TB dynamics. First, we tested the approach in a quasi-real setting. This allowed us to compare the implied values of the parameters with the actual ones. All the parameters, except  $\gamma$ , were precisely recovered. This further allowed making a reliable estimate of the basic reproduction number  $\mathcal{R}_0$ . These conclusions remained true, even in the case of the presence of noise in the observations, which demonstrated the robustness of the algorithm.

The reason why the error in the reconstruction of  $\gamma$  was higher than in the others was that the model was, to a large extent, insensitive to this parameter. This fact hindered the identification of  $\gamma$ , but on the other hand, this value was not crucial for the implied TB dynamics. Even with a large error in this value, the system would behave identically, thus reconstructing  $\gamma$  is of small importance.

In the real world, however, we do not know the "fair" values of the parameters, so we cannot directly assess the quality of their recovery. This is why we introduced the residual measure Equation (21). If the solution to the direct problems with the implied parameters mimics the observed dynamics, we can be confident in the parameter estimates. This is what we carried out in the real-world application with public data from Pakistan [36]. Measurements were only available for the currently infected people and those who had died from TB. From the 2000–2019 data, we arrived at a high transmission rate  $\beta$  and  $\mathcal{R}_0 > 1$ . This means that the current measures were insufficient to turn the tide. The strategies that were most efficient and have the minimal cost could be deduced with an optimal control approach.

This study contributed to the available knowledge in the manner in which the proposed model accounts for the distinctive features of the TB dynamics, without introducing unnecessary complexity, as well as being able to be successfully calibrated. Its ability to cope well with real data might be very beneficial in modeling, simulating, and forecasting the spread of TB, which are useful tools in fighting the disease.

## 7. Conclusions

This study dealt with a TB epidemic model. The whole population was divided into five compartments: susceptible, infected but not yet infectious, infectious, treated, and recovered, along with vital dynamics. The immunity gained is not lifelong and decays with time. Furthermore, the considered mechanisms for contracting the infection include slow and fast contamination due to mass action, endogenous reactivation, and exogenous reinfection. Furthermore, those treated and recovered could again become exposed or infectious, due to an incomplete treatment or waning immunity.

This new model extends the previous ones twofold. The two types of memory incorporated—the time lag for short memory and the fractional order of the derivatives for long memory—make the model better adjustable to real data. It is clear that the current level of infectiousness depends, not only to the immediately preceding number of infected, but also on a long history due to the latent period. Thus, applying fractional-order derivatives is suitable for epidemiological modeling in general.

Along with suggesting a population dynamics model and conducting a basic analysis, the other aim of this study was to propose a robust algorithm to recover important param-

eters. We noted that statistics are usually collected only for the (detected) infectious and people deceased from TB. This information was included in a quadratic cost functional, which was minimized to find the optimal values of the unknown parameters that mimic the empirical disease dynamics as much as possible.

The model was calibrated with real-world data, and the results indicated that it could accurately capture the behavior of the disease under different scenarios. Such studies highlight the crucial role of mathematical modeling in controlling the spread of infections and for taking appropriate measures to prevent and treat the disease. This model can be used as a tool to assess the effectiveness of different interventions, such as vaccination programs and screening policies. We believe that this work will contribute to the ongoing efforts to combat tuberculosis and improve public health worldwide.

There are many ways in which this investigation could be continued. Probably the most straightforward way to further develop this study would be to implement an optimal control framework. This would give insights into the proper control strategies to employ, while keeping the resources used at an acceptable level.

Moreover, the model parameters could be considered as time- and space-dependent function instead of constants. In addition, stochastics could be involved in the dynamics. More compartments could be included for vaccinated or hospitalized people. Furthermore, TB often interacts with other diseases, most notably HIV, and recently COVID-19. It would be interesting and useful to employ a model that encompasses such a relation. What is more, population heterogeneities such as age structure, spatial discrepancy, and others would be worth studying. Such approaches, combined with various advanced numerical methods, are useful in many fields of science besides epidemiological modeling.

**Funding:** This study was supported by the Bulgarian National Science Fund under Project KP-06-M62/1 “Numerical deterministic, stochastic, machine and deep learning methods with applications in computational, quantitative, algorithmic finance, biomathematics, ecology and algebra” from 2022 and by the National Program “Young Scientists and Postdoctoral Researchers-2”–Bulgarian Academy of Sciences.

**Data Availability Statement:** The data used for the study are freely available at [36].

**Acknowledgments:** The author is grateful to the anonymous referees for their useful suggestions and comments.

**Conflicts of Interest:** The author declares no conflict of interest. The funders had no role in the design of the study; in the collection, analyses, or interpretation of data; in the writing of the manuscript; or in the decision to publish the results.

## Abbreviations

The following abbreviations are used in this manuscript:

AC	Absolutely continuous
GMF	Generalized mean value formula
(M)TB	(Mycobacterium) tuberculosis
ODE	Ordinary differential equation(s)

## Appendix A. EE State

Let us recall that the EE state  $\mathcal{E}_1 = (S^*, E^*, I^*, T^*, R^*)$  Equation (10) is defined via Equation (11) and  $I^*$  implicitly is stated as the real positive root of  $\tilde{a}(I^*)^3 + \tilde{b}(I^*)^2 + \tilde{c}I^* + \tilde{d} = 0$  Equation (12). The coefficients are as follows:

$$\begin{aligned} \tilde{a} = & \beta^3(\delta^2\gamma\rho\zeta - \gamma h\rho\sigma_2 - \phi\gamma\rho\sigma_1 - \delta\gamma\rho\sigma_1 - \gamma\rho\sigma_1\sigma_2 - \delta\gamma h\rho\zeta + \delta\phi\gamma\rho\zeta + \delta\gamma\rho\sigma_2\zeta - \gamma h\rho\zeta \\ & - \phi\gamma\rho\zeta - \delta\gamma\rho\zeta - \gamma\rho\sigma_2\zeta - \gamma\rho\sigma_1\zeta + \delta\gamma\rho\zeta\zeta - \gamma\rho\zeta^2) \end{aligned}$$

$$\begin{aligned} \tilde{b} = & \beta^2 ( -\gamma\zeta^3 - \rho\zeta^3 - \delta\gamma\zeta^2 - \phi\gamma\zeta^2 - \gamma h\zeta^2 - \gamma k\zeta^2 - \delta\rho\zeta^2 - \phi\rho\zeta^2 - \gamma\rho\zeta^3 - \gamma\sigma_1\zeta^2 - \gamma\sigma_2\zeta^2 - h\rho\zeta^2 \\ & - \rho\sigma_1\zeta^2 - \rho\sigma_2\zeta^2 - \delta\gamma k\sigma_1 - \phi\gamma k\sigma_1 - \delta\gamma h\zeta - \gamma h k\sigma_2 - \phi\gamma h\zeta - \delta\gamma k\zeta - \phi\gamma k\zeta - \gamma h k\zeta - \delta\gamma\sigma_1\zeta \\ & - \gamma k\sigma_1\sigma_2 - \phi\gamma\sigma_1\zeta - \phi h\rho\zeta - \gamma h\sigma_2\zeta - \gamma k\sigma_1\zeta - \gamma k\sigma_2\zeta - \delta\rho\sigma_1\zeta - \phi\rho\sigma_1\zeta - \gamma\sigma_1\sigma_2\zeta - h\rho\sigma_2\zeta - \rho\sigma_1\sigma_2\zeta \\ & + \delta^2\gamma k\zeta - \delta\gamma\rho\zeta^2 - \phi\gamma\rho\zeta^2 - \gamma h\rho\zeta^2 + \delta\gamma\zeta^2\zeta + \delta^2\gamma\zeta\zeta - \gamma\rho\sigma_1\zeta^2 - \gamma\rho\sigma_2\zeta^2 + \delta\rho\zeta^2\zeta \\ & + \delta^2\rho\zeta\zeta + \delta\phi\gamma k\zeta - \delta\gamma h k\zeta + \delta\gamma k\sigma_2\zeta + \delta\phi\gamma\zeta\zeta + \delta\gamma k\zeta\zeta - \delta\gamma\rho\sigma_1\zeta - \phi\gamma\rho\sigma_1\zeta \\ & - \gamma h\rho\sigma_2\zeta + \delta\phi\rho\zeta\zeta + \delta\gamma\sigma_2\zeta\zeta - \delta h\rho\zeta\zeta - \gamma\rho\sigma_1\sigma_2\zeta + \delta\rho\sigma_2\zeta\zeta + \delta\gamma\rho\zeta^2\zeta + \delta^2\gamma\rho\zeta\zeta \\ & + \delta\gamma\rho\sigma_2\zeta\zeta + \delta\phi\gamma\rho\zeta\zeta - \delta\gamma h\rho\zeta\zeta ) + \beta^3\Lambda\gamma\rho m_3 \end{aligned}$$

$$\begin{aligned} \tilde{c} = & \beta ( -\delta\zeta^3 - \phi\zeta^3 - \gamma\zeta^4 - h\zeta^3 - k\zeta^3 - \rho\zeta^4 - \sigma_1\zeta^3 - \sigma_2\zeta^3 - \zeta^4 - \delta\gamma\zeta^3 - \delta\gamma\zeta^3 - \delta h\zeta^2 - \phi\gamma\zeta^3 - \delta k\zeta^2 \\ & - \phi k\zeta^2 - \gamma k\zeta^3 - h k\zeta^2 - \delta\rho\zeta^3 - \delta\sigma_1\zeta^2 - \phi\rho\zeta^3 - \phi\sigma_1\zeta^2 - \gamma\sigma_1\zeta^3 - \gamma\sigma_2\zeta^3 - h\rho\zeta^3 - h\sigma_2\zeta^2 - k\sigma_1\zeta^2 - k\sigma_2\zeta^2 \\ & + \delta\zeta^3\zeta - \rho\sigma_1\zeta^3 - \rho\sigma_2\zeta^3 - \sigma_1\sigma_2\zeta^2 + \delta^2\zeta^2\zeta - \phi h k\zeta - \delta k\sigma_1\zeta - \phi k\sigma_1\zeta - h k\sigma_2\zeta - k\sigma_1\sigma_2\zeta - \delta\gamma h\zeta^2 - \phi\gamma h\zeta^2 \\ & - \delta\gamma k\zeta^2 - \phi\gamma k\zeta^2 - \gamma h k\zeta^2 - \delta\gamma\sigma_1\zeta^2 - \phi\gamma\sigma_1\zeta^2 - \phi h\rho\zeta^2 - \gamma h\sigma_2\zeta^2 + \delta\phi\zeta^2\zeta - \gamma k\sigma_1\zeta^2 - \gamma k\sigma_2\zeta^2 \\ & + \delta\gamma\zeta^3\zeta + \delta k\zeta^2\zeta + \delta^2 k\zeta\zeta - \delta\rho\sigma_1\zeta^2 - \phi\rho\sigma_1\zeta^2 - \gamma\sigma_1\sigma_2\zeta^2 - h\rho\sigma_2\zeta^2 + \delta\rho\zeta^3\zeta + \delta\sigma_2\zeta^2\zeta - \rho\sigma_1\sigma_2\zeta^2 \\ & + \delta^2\gamma\zeta^2\zeta + \delta^2\rho\zeta^2\zeta - \delta\gamma k\sigma_1\zeta - \phi\gamma k\sigma_1\zeta - \gamma h k\sigma_2\zeta + \delta\phi k\zeta\zeta - \delta h k\zeta\zeta - \gamma k\sigma_1\sigma_2\zeta + \delta k\sigma_2\zeta\zeta \\ & + \delta\phi\gamma\zeta^2\zeta + \delta\gamma k\zeta^2\zeta + \delta^2\gamma k\zeta\zeta + \delta\phi\rho\zeta^2\zeta + \delta\gamma\sigma_2\zeta^2\zeta - \delta h\rho\zeta^2\zeta + \delta\rho\sigma_2\zeta^2\zeta + \delta\phi\gamma k\zeta\zeta - \delta\gamma h k\zeta\zeta + \delta\gamma k\sigma_2\zeta\zeta \\ & + \beta^2\Lambda(\rho\zeta^2 + \rho\sigma_2\zeta + c\gamma\zeta^2 + \delta\gamma k + \phi\gamma k + \gamma k\sigma_2 + \gamma k\zeta + \delta\rho\zeta + \phi\rho\zeta + c\delta\gamma\zeta + c\phi\gamma\zeta + c\gamma\sigma_2\zeta) \end{aligned}$$

$$\begin{aligned} \tilde{d} = & \beta\Lambda\zeta m_3(k + c\tilde{c}) \\ & + (\delta^2 k\zeta - \phi h k - \delta k\sigma_1 - \phi k\sigma_1 - h k\sigma_2 - k\sigma_1\sigma_2 + \delta\phi k\zeta - \delta h k\zeta + \delta k\sigma_2\zeta)\zeta^2 - (\delta h + \phi h + \delta k + \phi k + h k + \delta\sigma_1 + \phi\sigma_1 \\ & + h\sigma_2 + k\sigma_1 + k\sigma_2 + \sigma_1\sigma_2 - \delta\zeta(\delta + \phi + k + \sigma_2))\zeta^3 - (\delta + \phi + h + k + \sigma_1 + \sigma_2 - \delta\zeta)\zeta^4 - \zeta^5 \end{aligned}$$

## References

1. Kermack, W.O.; McKendrick, A.G. A contribution to the mathematical theory of epidemics. *Proc. R. Soc. Lond. Ser. A* **1927**, *115*, 700–721.
2. Hethcote, H.W. The mathematics of infectious diseases. *SIAM Rev.* **2000**, *42*, 599–653. [[CrossRef](#)]
3. Hethcote, H.W. Three Basic Epidemiological Models. In *Applied Mathematical Ecology*; Levin, S.A., Hallam, T.G., Gross, L.G., Eds.; Springer: Berlin/Heidelberg, Germany, 1989.
4. Waaler, H.; Geser, A.; Andersen, S. The use of mathematical models in the study of the epidemiology of tuberculosis. *Am. J. Public Health Nation's Health* **1962**, *52*, 1002–1013. [[CrossRef](#)]
5. Revelle, C.S.; Lynn, W.R.; Feldmann, F. Mathematical models for the economic allocation of tuberculosis control activities in developing nations. *Am. Rev. Respir.* **1967**, *96*, 893–909.
6. Blower, S.M.; McLean, A.R.; Porco, T.C.; Small, P.M.; Hopewell, P.C.; Sanchez, M.A.; Moss, A.R. The intrinsic transmission dynamics of tuberculosis epidemics. *Nat. Med.* **1995**, *1*, 815–821. [[CrossRef](#)]
7. Vynnycky, E.; Fine, P.E. The Natural History of Tuberculosis: The Implications of Age-Dependent Risks of Disease and the Role of Reinfection. *Epidemiol. Infect.* **1997**, *119*, 183–201. [[CrossRef](#)]
8. Dye, C.; Garnett, G.P.; Sleeman, K.; Williams, B.G. Prospects for Worldwide Tuberculosis Control under the WHO DOTS Strategy. *Lancet* **1998**, *352*, 1886–1891. [[CrossRef](#)] [[PubMed](#)]
9. Ziv, E.; Daley, C.L.; Blower, S. Early therapy for latent tuberculosis infection. *Am. J. Epidemiol.* **2001**, *153*, 381–385. [[CrossRef](#)] [[PubMed](#)]
10. Cohen, T.; Murray, M. Modeling epidemics of multidrug-resistant M.tuberculosis of heterogeneous fitness. *Nat. Med.* **2004**, *10*, 1117–1121. [[CrossRef](#)]
11. Basu, S.; Andrews, J.R.; Poolman, E.M.; Gandhi, N.R.; Shah, N.S.; Moll, A.; Moodley, P.; Galvani, A.P.; Friedland, G.H. Prevention of nosocomial transmission of extensively drug-resistant tuberculosis in rural South African district hospitals: An epidemiological modelling study. *Lancet* **2007**, *370*, 1500–1507. [[CrossRef](#)]
12. Trauer, J.M.; Denholm, J.T.; McBryde, E.S. Construction of a mathematical model for tuberculosis transmission in highly endemic regions of the Asia-Pacific. *J. Theor. Biol.* **2014**, *358*, 74–84. [[CrossRef](#)]
13. White, R.G.; Charalambous, S.; Cardenas, V.; Hippner, P.; Sumner, T.; Bozzani, F.; Mudzengi, D.; Houben, R.M.G.J.; Collier, D.; Kimerling, M.E.; et al. Evidence-informed policy making at country level: Lessons learned from the South African Tuberculosis Think Tank. *Int. J. Tuberc. Lung Dis.* **2018**, *22*, 606–613. [[CrossRef](#)]

14. Knight, G.M.; McQuaid, C.F.; Dodd, P.J.; Houben, R.M. Global burden of latent multidrug-resistant tuberculosis: Trends and estimates based on mathematical modelling. *Lancet Infect. Dis.* **2019**, *19*, 903–912. [CrossRef]
15. Ojo, M.M.; Peter, O.J.; Goufo, E.F.D.; Panigoro, H.S.; Oguntolu, F.A. Mathematical model for control of tuberculosis epidemiology. *J. Appl. Math. Comput.* **2023**, *69*, 69–87. [CrossRef]
16. Bekiryazici, Z. Sensitivity analysis and random dynamics for a mathematical model of tuberculosis transmission. *Commun. Stat. Simul. Comput.* **2023**, 1–13. [CrossRef]
17. Castillo-Chavez, C.; Song, B. Dynamical models of tuberculosis and their applications. *Math. Biosci. Eng.* **2004**, *1*, 361–404. [CrossRef] [PubMed]
18. Liu, L.; Zhao, X.-Q.; Zhou, Y. A tuberculosis model with seasonality. *Bull. Math. Biol.* **2010**, *72*, 931–952. [CrossRef] [PubMed]
19. Khan, M.A.; Fatmawati, F.; Bonyah, E.; Hammouch, Z.; Mifta Shaiful, E. A mathematical model of tuberculosis (TB) transmission with children and adults groups: A fractional model. *AIMS Math.* **2020**, *5*, 2813–2842.
20. Treibert, S.; Brunner, H.; Ehrhardt, M. Compartment models for vaccine effectiveness and non-specific effects for Tuberculosis. *Math. Biosci. Eng.* **2019**, *16*, 7250–7298. [CrossRef]
21. Selvam, A.; Sabarinathan, S.; Senthil Kumar, B.V.; Byeon, H.; Guedri, K.; Eldin, S.M.; Khan, M.I.; Govindan, V. Ulam-Hyers stability of tuberculosis and COVID-19 co-infection model under Atangana-Baleanu fractal-fractional operator. *Sci. Rep.* **2023**, *13*, 9012. [CrossRef] [PubMed]
22. Singh, R.; Rehman, A.U.; Ahmed, T.; Ahmad, K.; Mahajan, S.; Pandit, A.K.; Abualigah, L.; Gandomi, A.H. Mathematical modelling and analysis of COVID-19 and tuberculosis transmission dynamics. *Inform. Med. Unlocked* **2023**, *38*, 101235. [CrossRef]
23. Ojo, M.M.; Peter, O.J.; Goufo, E.F.D.; Nisar, K.S. A mathematical model for the co-dynamics of COVID-19 and tuberculosis. *Math. Comput. Simul.* **2023**, *207*, 499–520. [CrossRef] [PubMed]
24. Wallis, R.S. Mathematical models of tuberculosis reactivation and relapse. *Front. Microbiol.* **2016**, *7*, 669. [CrossRef] [PubMed]
25. Hattaf, K.; Rachik, M.; Saadi, S.; Tabit, Y.; Yousfi, N. Optimal control of tuberculosis with exogenous reinfection. *J. Appl. Math. Sci.* **2009**, *3*, 231–240.
26. Liu, J.; Zhang, T. Global stability for a tuberculosis model. *Math. Comput. Model.* **2011**, *54*, 836–845. [CrossRef]
27. Huo, H.F.; Zou, M.X. Modelling effects of treatment at home on tuberculosis transmission dynamics. *Appl. Math. Modell.* **2016**, *40*, 9474–9484. [CrossRef]
28. Khajanchi, S.; Das, D.K.; Kar, T.K. Dynamics of tuberculosis transmission with exogenous reinfections and endogenous reactivation. *Physica A* **2018**, *497*, 52–71. [CrossRef]
29. Khan, M.A.; Ahmad, M.; Ullah, S.; Farooq, M.; Gul, T. Modeling the transmission dynamics of tuberculosis in khyber pakhtunkhwa Pakistan. *Adv. Mech. Eng.* **2019**, *11*, 1687814019854835. [CrossRef]
30. Chinnathambi, R.; Rihan, F.A.; Alsakaji, H.J. A fractional-order model with time delay for tuberculosis with endogenous reactivation and exogenous reinfections. *Math. Meth. Appl. Sci.* **2019**, *44*, 8011–8025. [CrossRef]
31. Zhang, X.-H.; Ali, A.; Khan, M.A.; Alshahrani, M.Y.; Muhammad, T.; Islam, S. Mathematical analysis of the TB model with treatment via Caputo-type fractional derivative. *Discr. Dyn. Nat. Soc.* **2021**, *2021*, 9512371. [CrossRef]
32. Akossi, A.; Chowell-Puente, G.; Smirnova, A. Numerical study of discretization algorithms for stable estimation of disease parameters and epidemic forecasting. *Math. Biosci. Eng.* **2019**, *16*, 3674–3693. [CrossRef]
33. Georgiev, S.; Vulkov, L. Coefficient identification in a SIS fractional-order modelling of economic losses in the propagation of COVID-19. *J. Comput. Sci.* **2023**, *69*, 102007. [CrossRef] [PubMed]
34. Georgiev, S.; Vulkov, L. Numerical Coefficient Reconstruction of Time-Depending Integer- and Fractional-Order SIR Models for Economic Analysis of COVID-19. *Mathematics* **2022**, *10*, 4247. [CrossRef]
35. Brauer, F.; Castillo-Chavez, C.; Feng, Z. Mathematical Models in Epidemiology; In *Texts in Applied Mathematics*; Springer: Berlin/Heidelberg, Germany, 2019; Volume 69.
36. The World Bank Data. 2023. Available online: <https://data.worldbank.org/indicator/SH.TBS.DTEC.ZS?locations=PK> (accessed on 7 May 2023).
37. Baleanu, D.; Diethelm, K.; Scalas, E.; Trujillo, J.J. *Fractional Calculus. Models and Numerical Methods*; World Scientific: Singapore, 2017.
38. Kilbas, A.A.; Srivastava, H.M.; Trujillo, J.J. *Theory and Applications of Fractional Differential Equations in: North-Holland Mathematics Studies*; Elsevier Science B.V: Amsterdam, The Netherlands, 2006; Volume 204.
39. Lin, W. Global existence theory and chaos control of fractional differential equations. *J. Math. Anal. Appl.* **2007**, *332*, 709–726. [CrossRef]
40. Diekmann, O.; Heesterbeek, J.A.P.; Metz, J.A.J. On the definition and the computation of the basic reproduction ratio  $R_0$  in models for infectious diseases. *J. Math. Biol.* **1990**, *35*, 503–522.
41. Chowell, G.; Brauer, F. The basic reproduction number of infectious diseases: Computation and estimation using compartmental epidemic models. In *Mathematical and Statistical Estimation Approaches in Epidemiology*; Chowell, G., Hyman, J.M., Bettencourt, L.M.A., Castillo-Chavez C., Eds.; Springer: Dordrecht, The Netherlands, 2009; pp. 1–30.
42. van den Driessche, P.; Watmough, J. Reproduction numbers and sub-threshold endemic equilibria for compartmental models of disease transmission. *Math. Biosci.* **2002**, *180*, 29–48. [CrossRef] [PubMed]

43. Li, C.; Tao, C. On the fractional Adams method. *Comput. Math. Appl.* **2009**, *58*, 1573–1588. [[CrossRef](#)]
44. Banks, H.T.; Dediu, S.; Ernstberger, S. Sensitivity functions and their uses in inverse problems. *J. Inverse Ill-Posed Probl.* **2008**, *15*, 683–708. [[CrossRef](#)]

**Disclaimer/Publisher's Note:** The statements, opinions and data contained in all publications are solely those of the individual author(s) and contributor(s) and not of MDPI and/or the editor(s). MDPI and/or the editor(s) disclaim responsibility for any injury to people or property resulting from any ideas, methods, instructions or products referred to in the content.